

Evidence for a strain-induced variation of the magnetic moment in epitaxial Cu/Ni/Cu/Si(100) structures

Jaeyong Lee, G. Lauhoff, M. Tselepi, S. Hope, P. Rosenbusch, and J. A. C. Bland
Cavendish Laboratory, University of Cambridge, Cambridge CB3 0HE, United Kingdom

H. A. Dürr and G. van der Laan
Daresbury Laboratory, Warrington WA4 4AD, United Kingdom

J. Ph. Schillé and J. A. D. Matthew
Department of Physics, York University, York YO1 5DD, United Kingdom

(Received 24 February 1997)

We have studied the magnetic moment and in-plane strain in epitaxial Cu/Ni/Cu/Si(100) structures by varying both the Ni and Cu buffer layer thickness. We find a sharp reduction in magnetic moment with increasing Ni lattice strain. Our structural and temperature-dependent studies exclude interdiffusion, interface roughness, and a decreased Curie temperature as possible causes of the reduced moment, but reveal a strong correlation between the strain and magnetic moment in Cu/Ni/Cu structures. [S0163-1829(97)05322-8]

The atomic magnetic moment is one of the most elemental quantities in magnetism. Since the theoretical predictions of enhanced magnetic moments^{1,2} in ultrathin transition-metal films, there has been strong interest in experimental studies.³ For example, an enhanced orbital moment associated with the reduced interface symmetry has been proposed⁴ and observed in ultrathin Co films with perpendicular magnetic anisotropy (PMA).⁵ These studies clearly establish the importance of the interface in modifying the magnetic moment. However, strain is also a very important property of epitaxial thin films, giving rise to a magnetic anisotropy through the magnetoelastic interaction. In epitaxial Ni/Cu(001) PMA occurs for a surprisingly large thickness range⁶⁻⁸ and is explained by magnetoelastic anisotropy caused by the in-plane lattice mismatch between Ni and Cu. However, the strain dependence of the magnetic moment has not been well studied experimentally in epitaxial transition-metal films.

In this paper we report the observation of an unusual variation of magnetic moment and strain in epitaxial Cu/NiCu/Si(001) structures. Three different step-wedged samples (see Table I) were prepared for this study: Sample *A* shows a large variation of strain and magnetic moment with Ni layer thickness. From sample *B* we have observed a clear Ni magnetic moment variation correlated with a strain variation of the Cu buffer wedge. Sample *C* was prepared to study the possibility of roughness-dependent interdiffusion or a possible temperature dependence of the magnetic moment. We demonstrate that the observed magnetic moment variation in these structures is not due to impurities, interdiffu-

sion, interface roughness, or a reduced Curie temperature but suggests a strong correlation between strain and magnetic moment per atom in the Ni film.

Si(001) substrates were degreased and etched in diluted HF solution for 12 min prior to loading into the growth chamber. After an overnight bake-out the Si substrate was annealed for 2 h at ~ 200 °C to improve the reflection high-energy electron-diffraction (RHEED) pattern of the Si. The chamber base pressure was 1×10^{-9} mbar for sample *A* and *B* and increased to 5×10^{-9} mbar during growth. The base pressure for sample *C* was below 5×10^{-10} mbar and below 3×10^{-9} mbar during growth. Cu buffer layers were grown at 10–15 Å/min using an electron-beam-heated Mo crucible and the epitaxial Ni film at 1.5–2 Å/min by electron-beam evaporation. The growth temperature was maintained at room temperature or at least the substrate was not heated intentionally during growth. Step widths are >3 mm for all structures. A Cu capping layer was further deposited for *ex situ* measurements. The film thickness was estimated using a quartz crystal monitor close to the sample position. A 5% atomic concentration of O and C was found for sample *A*, and a trace of C was found for sample *B* by Auger electron spectroscopy (AES) as shown in Fig. 1(a). The AES taken after the complete Cu/Si(001) shows no contaminants on the 2000 Å Cu part within the noise level and traces of C and O on the 600 Å Cu side as shown in Fig. 1(b), which were too small to quantify (sample *C*). The AES measurements after the first 3 Å Ni film show no contaminants.

The RHEED images were recorded using a CCD camera and a line shape analysis of the RHEED streaks was used to

TABLE I. Three wedged samples and their specification.

Sample	Specification
Sample <i>A</i>	30 Å Cu/(30, 60, 90, and 150 Å) Ni/600 Å Cu/Si(001)
Sample <i>B</i>	30 Å Cu/50 Å Ni/(600, 1000, 1500, and 2000 Å) Cu/Si(001)
Sample <i>C</i>	50 Å Cu/30 Å Ni/(600 and 2000 Å) Cu/Si(001)

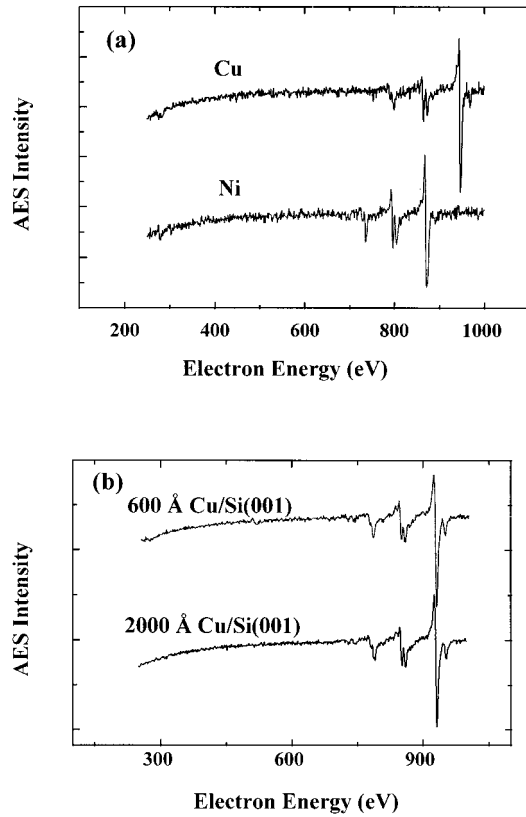


FIG. 1. (a) Auger spectra of sample B taken after the growth of 600 Å Cu/Si(001) and 50 Å Ni/600 Å Cu/Si(001). (b) Auger spectra of sample C taken after the completion of the 2000 Å Cu buffer.

evaluate the lateral strain. RHEED patterns taken from thick Cu buffers and subsequent Ni layers are sharper than those from the 600 Å Cu buffer. Also the RHEED patterns indicate that three-dimensional epitaxial growth occurs along the [001] direction with the Cu cubic axes rotated in-plane by 45° with respect to the Si(001) principal axis.⁶ The 600 Å thick Cu(001) film displays a very weak polycrystalline component.

The x-ray magnetic circular dichroism (XMCD) experiments were performed at beam line 1.1 of the synchrotron radiation source at Daresbury (UK) with 80% circularly polarized x rays. The $L_{2,3}$ x-ray-absorption spectra (XAS) were obtained at room temperature in the total electron-yield mode where the sample current is recorded as a function of photon energy. During the measurement the sample was magnetically saturated in a 1 T field perpendicular to the sample surface. The circular magnetic dichroism signal, $\sigma_M = \sigma^+ - \sigma^-$, is the difference between the XAS measured with the circular polarization of the beam fixed and the sample magnetization oriented first parallel (σ^+) and then antiparallel (σ^-) to the propagation vector of the light by reversing the direction of the applied field. The average of the two spectra corresponds to a combination of the linearly polarized and isotropic XAS spectrum.

The in-plane nearest-neighbor distances (NN_{in}) for Cu and Ni vs thickness from sample A are shown in Fig. 2 with the corresponding bulk values. The values of NN_{in} of Cu do not reach that of bulk Cu in the thickness range studied. The

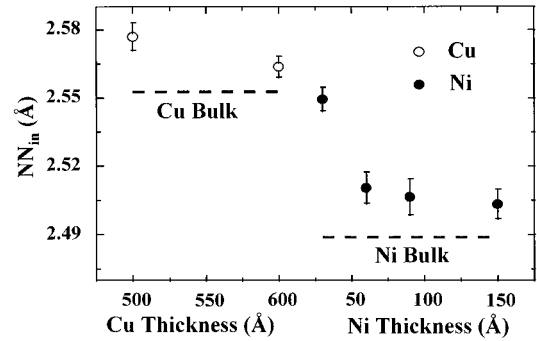


FIG. 2. In-plane nearest neighbor distances (NN_{in}) of Cu and Ni films determined by RHEED during the growth of sample A. The NN_{in} of bulk Cu and Ni are shown for comparison.

value of NN_{in} for the Ni film shows a dramatic change with thickness. The 30 Å Ni film is found to be strongly strained.

Figure 3 shows the normalized XAS and the XMCD difference spectra for sample A. The two features (marked A and A') located at about 6 eV above the L_3 and L_2 white lines in the XAS spectra have been previously reported⁹ and discussed¹⁰ together with the two features in the dichroism spectra at about 4 eV above (marked B and B'). It is clear that the XMCD signal increases with Ni thickness. Figure 4 shows the thickness dependence of Ni NN_{in} and atomic magnetic moment determined by XMCD-sum rules¹¹ for sample A. A clear trend is seen in each case, with a rapid initial change in magnetic moment and NN_{in} with thickness leveling off around 90 Å Ni. This suggests a strong correlation between strain and magnetic moment.

In order to verify this correlation and to exclude the possible effect of impurities¹² on our observation of a magnetic moment variation we have prepared sample B which has a step-wedged Cu buffer layer with a constant thickness Ni layer and a Cu capping layer. Based on the results shown in Fig. 2, we can expect that the Cu strain changes with increasing Cu buffer thickness even beyond 600 Å Cu buffer thickness and as a result the strain of the overlying epitaxial Ni films is expected to change in this structure. Figure 5 shows a clear trend of the Cu buffer thickness dependence of NN_{in} for Cu, normalized polar magneto-optic Kerr effect (MOKE) height, and Ni atomic magnetic moment per Ni determined from the XMCD experiment, such that the mag-

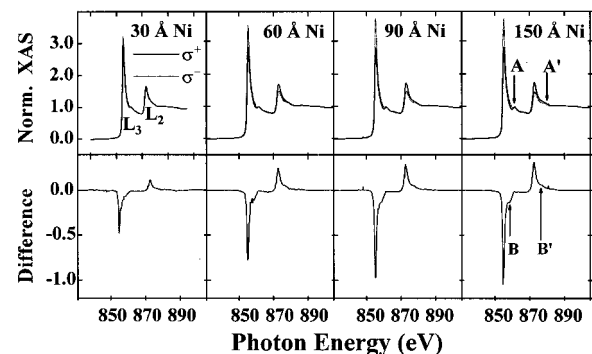


FIG. 3. Normalized XAS and their difference spectra of sample A with Ni thickness. The intensity of the difference spectra decreases with decreasing Ni thickness.

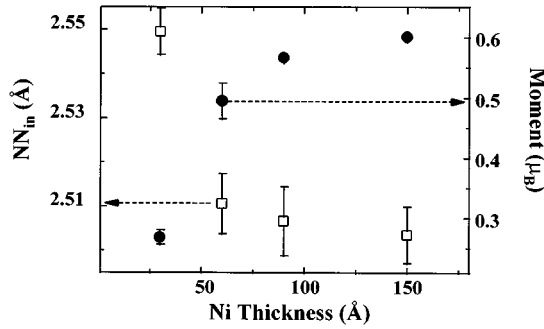


FIG. 4. NN_{in} of Ni and atomic moments of sample A. The atomic moments show strong variation between 30 and 60 Å Ni thickness which is the thickness range of strong variation of Ni lateral strain.

netic moment of this system is increasing with decreasing Cu strain. For this sample, polar MOKE measurements, which confirmed the 100% remanence of sample B, is an especially powerful tool because the total film thickness at each position exceeds the probing depth (~ 200 Å) of MOKE and therefore the height of the polar loop should be directly related to the local magnetization throughout the wedge structure. Experimental errors prevent us from directly determining the strain in the Ni layer, but it is reasonable to assume that the strain variation in the Ni layer follows the strain variation in Cu.

A magnetically dead layer ($Ni_{40}Cu_{60}$) caused by Cu interdiffusion may explain our observations of a decreased magnetic moment since Cu may interdiffuse into Ni layer during Ni growth due to the lower surface free energy of Cu and XMCD has a limited probing depth. From the fit to the L_3 edge jump of sample A we found that the probing depth of XMCD in our geometry is 35 ± 5 Å. In order to account for the magnetic moment of the 30 and 60 Å Ni films in sample A, at least a 19 Å thick magnetically dead layer would be needed, which should give an AES ratio of *LMM* Cu (922 eV) to Ni (849 eV) of 0.22. But the AES spectrum taken

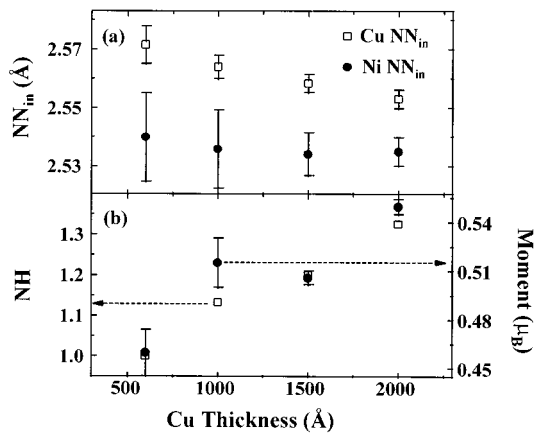


FIG. 5. Several parameters versus Cu buffer thickness of sample B. (a) NN_{in} of Cu and Ni. (b) Normalized heights (NH) of the polar MOKE loop (left axis), where the height of the polar MOKE loop at each thickness is divided by the height obtained at 600 Å Cu, and the magnetic moments of Ni determined by XMCD-sum rules (right axis).

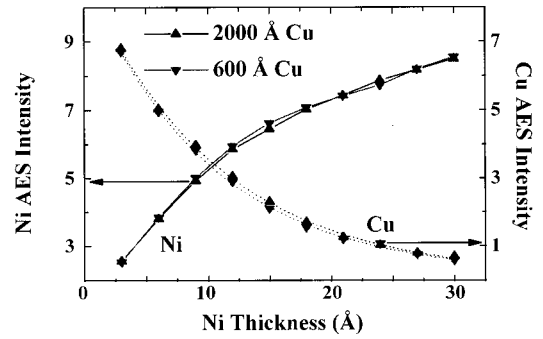


FIG. 6. Auger *LMM* intensities of Ni (left) and Cu (right) measured during Ni film growth (sample C). Upright symbols represent signals from the 2000 Å Cu side and downright symbols from the 600 Å Cu side. The dotted lines passing through the Cu data points are fitted curves, assuming an exponential decay of the Cu intensities.

after growing 30 Å Ni of sample A did not show any measurable Cu peaks compared with Ni. Polarized neutron reflection measurements on the same system also did not show any evidence of a localized magnetically dead layer of ~ 20 Å.¹³ Moreover, in order to explain the magnetic moment difference shown in Fig. 5(b), the Ni film on 600 Å Cu should have a magnetically dead layer 11 ± 2 Å thicker than the Ni on the 2000 Å Cu buffer, which would imply a very strong dependence of interdiffusion on roughness. Therefore we have studied the possibility of roughness-dependent interdiffusion by taking AES during Ni growth on a two-step Cu buffer wedge (sample C) as shown in Fig. 6. The AES taken after successive deposition of 3 Å Ni allow us to test the possibility of strongly roughness-dependent interdiffusion. The height of Ni and Cu Auger intensities from the 600 and 2000 Å Cu buffer layers are the same within experimental errors, suggesting that there is no roughness-dependent interdiffusion. The values for the mean free paths for Cu Auger electrons of 10.8 ± 45 Å for the 2000 Å Cu buffer and 10.0 ± 0.39 Å for the 600 Å Cu buffer obtained by assuming an exponential decay of Cu intensity are in good agreement. This clearly shows that our observations of a changing magnetic moment are not due to interdiffusion. We have made temperature-dependent measurements using a superconducting quantum interference device on the 600 Å Cu buffer part of sample C and found that the magnetic moment at 300 K is reduced by only $14 \pm 5\%$ from the value of 50 K, which means that the Curie temperature of this structure is far above room temperature as expected¹⁴ for this thickness (≥ 30 Å).

Our findings of a Ni moment variation apparently differ from earlier work at first sight, in which O'Brien and Tonner¹⁵ have observed that the normalized XMCD signal in the remanent state for Si grown on single crystal Cu(001) is constant for the Ni thickness ranges of 12–75 ML. We now consider two possible mechanisms which could give rise to this difference.

Firstly, our Ni films are grown on a Cu buffer layer, which is expected to have a rough surface compared to a well-treated Cu(001) single crystal. But in order to explain the magnetic moment difference observed in sample B as a result of surface roughness, the 50 Å Ni on 600 Å Cu should

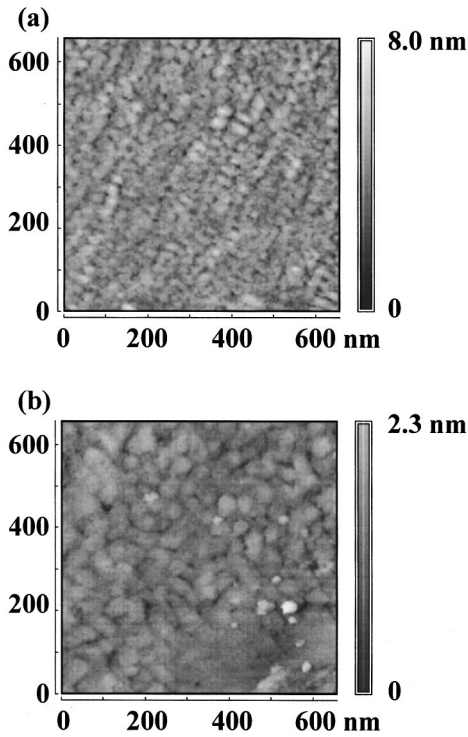


FIG. 7. Scanning tunneling microscopy images of sample C from (a) 600 Å and (b) 2000 Å Cu buffer side taken after the 50 Å Cu capping layer.

have an 11 times larger Ni-Cu interface area than the 50 Å Ni on 2000 Å Cu if we use the theoretically determined value of $0.39\mu_B$ for 1 ML/Cu(001),¹⁶ and include the effect of the limited probing depth for XMCD. This means that for every 1 Å lateral variation an ~ 11 Å vertical variation is needed, which is a very unrealistic interface shape. This view is confirmed by scanning tunneling microscopy images of sample C taken after Cu capping as shown in Fig. 7. The average island size of the thin Cu buffer side is 400 ± 20 Å in lateral scale with ~ 20 Å vertical variation and that of the thick Cu buffer side is 580 ± 30 Å in lateral scale with the 12 Å vertical variation.

Secondly, the strain in our samples is likely to be greater than that in Ni grown on a Cu single crystal. We have shown

that the magnetic moment variation of the Ni is always correlated with the strain variation in the Ni layer, either directly (Fig. 4) or indirectly via the Cu buffer (Fig. 5). We notice that all Ni films studied here were capped with at least 30 Å Cu. The effect of a Cu capping layer on the strain in the Ni is such that the critical thickness (t_c) for coherent growth increases from 15 Å in Ni/Cu(001) to 42 Å in Cu/Ni/Cu(001).¹⁷ In the incoherent growth region above t_c , the residual strain ε can be expressed as $\varepsilon = \eta t_c / t$, where η is the lattice misfit.¹⁸ Therefore we can expect that the Cu capping layer not only increases the value of t_c but also the strain in the Ni film in the incoherent growth region. Based on this effect, we can qualitatively estimate how much strain difference exists between the Ni films with/without Cu capping. In the incoherent region, a 12 ML thickness Ni layer on Cu(001), which is the maximum thickness up to which a sharp magnetic moment variation occurs,¹⁵ may experience almost the same strain as a Cu/60 Å Ni/Cu(001) structure does; this is the same Ni thickness range in which we have observed a dramatic magnetic moment variation for sample A. Based on the above argument we conclude that our structures are experiencing additional strain due to the presence of the Cu capping layer in addition to the strain measured by *in situ* RHEED. We believe that a reduced relaxation of the strain in our films is the reason why we observed a magnetic moment variation over a wide thickness range (30–90 Å) of Ni.

In summary, we have observed a dramatic variation in magnetic moment and the in-plane strain with both Ni and Cu buffer layer thickness. Our structural and temperature-dependent studies exclude the possibility of roughness-dependent interdiffusion or decreased Curie temperature as the cause of the dramatic magnetic moment variation in our samples. Our observations therefore suggest an unexpectedly strong correlation between strain and magnetic moment in Cu/Ni/Cu structures, though we cannot rule out other possibilities, such as a volume change in the distorted Ni unit cell.

We acknowledge the use of the superconducting magnetic facility under EPSRC Grant No. GR J82195. We would also like to thank the staff from York University and Daresbury Laboratory and particularly Dr. I. W. Kirkman for his help at the beamline and for writing the XMCD data acquisition software. We thank the EPSRC for financial support.

¹R. Richter, J. G. Gay, and J. R. Smith, Phys. Rev. Lett. **54**, 2704 (1985).

²C. L. Fu, A. J. Freeman, and T. Oguchi, Phys. Rev. Lett. **54**, 2700 (1985).

³J. A. C. Bland, R. D. Bateson, B. Heinrich, Z. Celinski, and H. J. Lauter, J. Magn. Magn. Mater. **104-107**, 1909 (1992); J. A. C. Bland, C. Daboo, B. Heinrich, Z. Celinski, and Bateson, Phys. Rev. B **51**, 258 (1995).

⁴G. H. O. Daalderop, P. J. Kelly, and M. F. H. Schuurmans, Phys. Rev. B **44**, 12 054 (1991).

⁵Y. Wu, J. Stöhr, B. D. Hermsmeier, M. G. Samant, and D. Weller, Phys. Rev. Lett. **69**, 2307 (1992).

⁶R. Naik, C. Kota, J. S. Payson, and G. L. Dunifer, Phys. Rev. B **48**, 1008 (1993); R. Naik, A. Poli, D. McKague, A. Lukaszew,

and L. E. Wenger, *ibid.* **51**, 3549 (1995).

⁷G. Bochi, H. J. Hug, D. I. Paul, B. Stiefel, A. Moser, I. Parashikov, H.-J. Güntherodt, and R. C. O'Handley, Phys. Rev. Lett. **75**, 1839 (1995).

⁸Chin-An Chang, J. Appl. Phys. **68**, 4873 (1990).

⁹N. V. Smith, C. T. Chen, F. Sette, and L. F. Mattheiss, Phys. Rev. B **46**, 1023 (1992); C. T. Chen, N. V. Smith, and F. Sette, *ibid.* **43**, 6785 (1991).

¹⁰G. van der Laan and B. T. Thole, J. Phys. Condens. Matter **4**, 4181 (1992).

¹¹B. T. Thole, P. Carra, F. Sette, and G. van der Laan, Phys. Rev. Lett. **68**, 1943 (1992); P. Carra, B. T. Thole, M. Altarelli, and X. Wang, *ibid.* **70**, 694 (1993).

¹²M. Donath, F. Passek, and V. Dose, Phys. Rev. Lett. **70**, 2802

- (1993); M. donath, Surf. Sci. **287**, 722 (1993); F. May, M. Tischer, D. Arvanitis, J. Hunter Dunn, H. Henneken, H. Wende, R. Chauvistré, N. Mårtensson, and K. Baberschke, Phys. Rev. B **53**, 1076 (1996).
- ¹³S. Hope, J. Lee, P. Rosenbusch, G. Lauhoff, S. A. C. Bland, A. Ercole, D. Bucknall, J. Penfold, H. J. Lauter, V. Lauter, and R. Cubitt, Phys. Rev. B **55**, 11422 (1997).
- ¹⁴F. Huang, M. T. Kief, G. J. Mankey, and R. F. Willis, Phys. Rev. B **49**, 3962 (1994).
- ¹⁵W. L. O'Brien and B. P. Tonner, Phys. Rev. B **49**, 15 370 (1994).
- ¹⁶D. S. Wang, A. J. Freeman, and H. Krakauer, Phys. Rev. B **26**, 1340 (1982); O. Hjørstam, J. Trygg, J. M. Wills, B. Johansson, and O. Eriksson, *ibid.* **53**, 9204 (1996).
- ¹⁷R. Jungblut, M. T. Johnson, J. aan de Stegge, A. Reinders, and F. J. A. Broeder, J. Appl. Phys. **75**, 6424 (1994).
- ¹⁸C. Chappert and P. Bruno, J. Appl. Phys. **64**, 5736 (1988).